JVI Journals.ASM.org

HSP90 Protects the Human T-Cell Leukemia Virus Type 1 (HTLV-1) Tax Oncoprotein from Proteasomal Degradation To Support NF-κB Activation and HTLV-1 Replication

Linlin Gao,[a] Edward William Harhaj[b]

Graduate Program in Cancer Biology, Sylvester Comprehensive Cancer Center, The University of Miami Miller School of Medicine, Miami, Florida, USA[a]; Department of Oncology, Sidney Kimmel Comprehensive Cancer Center, Johns Hopkins School of Medicine, Baltimore, Maryland, USA[b]

Human T-cell leukemia virus type 1 (HTLV-1) is the causative agent of adult T-cell leukemia (ATL) and HTLV-1-associated myelopathy/tropical spastic paraparesis (HAM/TSP). The HTLV-1 genome encodes the Tax protein that plays essential regulatory roles in HTLV-1 replication and oncogenic transformation of T lymphocytes. Despite intensive study of Tax, how Tax interfaces with host signaling pathways to regulate virus replication and drive T-cell proliferation and immortalization remains poorly understood. To gain new insight into the mechanisms of Tax function and regulation, we used tandem affinity purification and mass spectrometry to identify novel cellular Tax-interacting proteins. This screen identified heat shock protein 90 (HSP90) as a new binding partner of Tax. The interaction between HSP90 and Tax was validated by coimmunoprecipitation assays, and colocalization between the two proteins was observed by confocal microscopy. Treatment of HTLV-1-transformed cells with the HSP90 inhibitor 17-DMAG elicited proteasomal degradation of Tax in the nuclear matrix with concomitant inhibition of NF-κB and HTLV-1 long terminal repeat (LTR) activation. Knockdown of HSP90 by lentiviral shRNAs similarly provoked a loss of Tax protein in HTLV-1-transformed cells. Finally, treatment of HTLV-1-transformed cell lines with 17-DMAG suppressed HTLV-1 replication and promoted apoptotic cell death. Taken together, our results reveal that Tax is a novel HSP90 client protein and HSP90 inhibitors may exert therapeutic benefits for ATL and HAM/TSP patients.

The human T-cell leukemia virus type 1 (HTLV-1) was the first identified human retrovirus associated with a malignancy (1). Currently, there are four distinct subtypes of HTLV (1–4); however, HTLV-1 exhibits the greatest pathogenicity. HTLV-1 is linked to the genesis of a fatal malignancy of $CD4^+CD25^+$ T lymphocytes known as adult T-cell leukemia (ATL). About 2 to 5% of all HTLV-1-infected patients develop ATL after a long latent period lasting decades, which then progresses rapidly and is highly resistant to current chemotherapeutic regimens (2). HTLV-1 infection is also associated with inflammatory diseases, most notably the neurological disorder HTLV-1-associated myelopathy/tropical spastic paraparesis (HAM/TSP). Although disease occurs in only a small percentage of HTLV-1-infected individuals, high proviral load is a major risk factor for disease progression (3).

The HTLV-1 genome encodes a 40-kDa regulatory protein, Tax, which controls HTLV-1 replication and also promotes the oncogenic transformation of T lymphocytes (4, 5). Tax modulates the activation of host signaling pathways and cell cycle regulators to sustain T-cell proliferation and survival, ultimately resulting in immortalization (6). One of the main targets of Tax essential for cell transformation is the NF-κB pathway (7). NF-κB is an evolutionarily conserved transcription factor family composed of heterodimeric proteins consisting of p65 (RelA), c-Rel, RelB, p50, and p52 (8). NF-κB is sequestered in the cytoplasm by a family of ankyrin-repeat-containing inhibitory proteins, most notably IκBα, which is induced by NF-κB and suppresses signaling in a negative-feedback loop (9). A large variety of stimuli, including stress signals, proinflammatory cytokines, and virus infection activate the IκB kinase (IKK) complex, consisting of the catalytic subunits IKKα and IKKβ and the regulatory subunit NEMO (also known as IKKγ) (10). IKKβ phosphorylates IκB proteins to trigger ubiquitin-dependent proteasomal degradation to allow NF-κB to enter the nucleus and activate target genes (11). Tax activates IKK and NF-κB persistently by interacting with NEMO (12, 13); however, the exact mechanism of IKK activation by Tax remains poorly understood. Tax mutants defective in NF-κB activation are impaired in the immortalization of primary T cells (14). In addition, NF-κB plays a key survival role in HTLV-1-transformed cell lines and patient-derived ATL cells (15).

Tax plays an essential role in HTLV-1 replication by activating transcription from the viral long terminal repeats (LTR) (16). Tax activates the LTR mainly through the cyclic AMP (cAMP) response element binding protein/activating transcription factor (CREB/ATF) pathway. Tax interacts with CREB dimers and increases the affinity of CREB for three highly homologous 21-bp Tax-responsive elements in the LTR (17). The transcriptional coactivators CREB-binding protein (CBP) and p300 are also recruited to the CREB-Tax 21-bp repeat complex and play a key role in chromatin remodeling (18). Through the concerted action of these host transcription factors and coactivator proteins, Tax strongly activates HTLV-1 gene expression.

Heat shock protein 90 (HSP90) is an evolutionarily conserved molecular chaperone that plays an essential role in the folding, maturation, and trafficking of nascent polypeptides (19). HSP90 substrates or clients play a critical role in growth control and cell survival, many of which have been implicated in tumorigenesis

Received 19 July 2013 **Accepted** 1 October 2013
Published ahead of print 9 October 2013
Address correspondence to Edward William Harhaj, eharhaj1@jhmi.edu.

doi:10.1128/JVI.02006-13

(20, 21). HSP90 is comprised of three domains: an amino (N)-terminal domain with ATP-binding and ATPase activity that assists in client protein folding, a central domain involved in client protein recognition, and a carboxyl (C)-terminal domain that contains a dimerization motif and binding sites for other cochaperones (22). HSP90 catalyzes the hydrolysis of ATP to provide energy for folding client proteins into their correct three-dimensional conformations (23). Geldanamycin (GA) and its derivative, 17-demethylaminoethylamino-17-demethoxygeldanamycin (17-DMAG), are potent HSP90 inhibitors and bind HSP90 at the N-terminal ATP-binding domain to inhibit its protein chaperone activity, resulting in protein misfolding and subsequent degradation (24). The HSP90 inhibitor 17-DMAG and other small-molecule inhibitors of HSP90 have been shown to exert potent antitumor activity in preclinical models and have entered clinical trials for various cancers (25).

In this study, we provide evidence that HTLV-1 Tax is a bona fide client protein of HSP90. Tax interacts with HSP90, and treatment of Tax-expressing cells with 17-DMAG elicited Tax proteasomal degradation and attenuation of Tax-induced HTLV-1 LTR and NF-κB activation. The inhibition of Tax by 17-DMAG suppressed viral replication and triggered apoptotic cell death of HTLV-1-transformed cell lines. These data suggest that HSP90 inhibitors may exert therapeutic benefits for ATL and HAM/TSP patients.

MATERIALS AND METHODS

Biological reagents, plasmids, and antibodies. Human embryonic kidney cells (HEK 293T) were purchased from ATCC. The HTLV-1-transformed cell lines C8166, MT-2, and MT-4 were described previously (26). HEK 293T cells were cultured in Dulbecco's modified Eagle's medium (DMEM); C8166, MT-2, and MT-4 cells were cultured in RPMI medium. Medium was supplemented with fetal bovine serum (10%) and penicillin-streptomycin (1%). Expression vectors encoding pCMV4-Tax, Tax M22, Tax M47, green fluorescent protein (GFP)-Tax, HTLV-1 LTR-Luc, and NF-κB Luc. were described previously (27, 28). Flag-Tax was a gift from U. Bertazzoni (29). HA-HSP90 beta was from William Sessa and obtained from Addgene (plasmid 22487). HTLV-1 ACH.wt and ACH.M22 proviral clones were generous gifts from Lee Ratner (30). The monoclonal anti-Tax antibody was prepared from a Tax hybridoma (168B17-46-34) received from the AIDS Research and Reference Program, NIAID, National Institutes of Health. Alexa Fluor 555-conjugated donkey anti-mouse IgG and Alexa Fluor 488-conjugated donkey anti-rabbit IgG were purchased from Life Technologies. The FLAG M2 antibody was purchased from Sigma. NEMO, IκBα, p50, Sp1, CD25, and lactate dehydrogenase (LDH) antibodies were from Santa Cruz Biotechnology. IKKα, IKKβ, HSP90, CREB, TBK1, p65, AKT, GM-130, lamin B2, poly(ADP-ribose) polymerase (PARP), caspase 3, lysine 48 (K48), and lysine 63 (K63) linkage-specific polyubiquitin antibodies were from Cell Signaling Technology. 20S proteasome antibody was from Enzo Life Sciences. The monoclonal hemagglutinin (HA) antibody (12CA5) was from Roche Applied Science. HTLV-1 p19 antibody was from ZeptoMetrix. β-Actin antibody was purchased from Abcam. DAPI (4′,6-diamidino-2-phenylindole) and MG-132 were purchased from EMD Biosciences. Bafilomycin A1 and ammonium chloride were purchased from Sigma.

Transfections and reporter assays. 293T cells were transiently transfected with GenJet In Vitro DNA Transfection Reagent (SignaGen Laboratories). Luciferase reporter assays were performed 24 h after DNA transfection, unless otherwise indicated, using the Dual-Glo luciferase assay system (Promega). Firefly luciferase values were normalized based on the *Renilla* luciferase internal control values. Luciferase values are presented as "fold induction" compared to the control transfected with empty vector.

MS. Flag-tagged Tax was cloned into the pNTAP-vector (InterPlay Mammalian tandem affinity purification system; Agilent) to yield pNTAP-Tax. 293T cells were transfected with pNTAP or pNTAP-Tax, and lysates were prepared 48 h after transfection. Tax and associated proteins were purified by a two-step immunoaffinity method, first by incubation with streptavidin resin and streptavidin binding buffer. Next, washed and eluted proteins were incubated with calmodulin resin and calmodulin binding buffer, followed by washing and elution with calmodulin binding buffer and calmodulin elution buffer, respectively. Purified proteins were resolved on a 10% SDS-PAGE gel and stained using the SilverQuest silver staining kit (Life Technologies). Bands visible in the lysates from pNTAP-Tax-transfected cells, but not pNTAP vector, were excised and subjected to mass spectrometry (MS) at the mass spectrometry/proteomic facility at Johns Hopkins School of Medicine. Proteins in gel bands were reduced in 5 mM dithiothreitol (DTT) at 60°C for 45 min, alkylated with 20 mM iodoacetomide at room temperature for 20 min in the dark, and proteolyzed with 10 ng trypsin (Promega)/μl overnight at 37°C as previously described (31). Extracted peptides were analyzed by liquid chromatography-tandem mass spectrometry (LC-MS/MS) analysis using an LTQ Orbitrap Velos mass spectrometer interfaced with a nano-Acquity ultrahigh-pressure liquid chromatography (UPLC) system. Peptide sequences were identified from isotopically resolved masses in MS and MS/MS spectra extracted with and without deconvolution using Thermo Scientific Xtract and MS2-processor software with Proteome Discoverer 1.3 (Thermo Scientific) software configured with the Mascot version 2.1 search node. Data were searched against RefSeq version 2012, assuming human species with oxidation on methionine and deamidation of asparagine and glutamine as variable modifications and carbamidomethyl on cysteine as a fixed modification. Mascot search results were also imported into Scaffold (version 3.6.5) to validate MS/MS-based peptide and protein identifications.

Immunoblotting, coimmunoprecipitations, and ubiquitination assays. Whole-cell lysates were generated by lysing cells in RIPA buffer (50 mM Tris-Cl [pH 7.4], 150 mM NaCl, 1% NP-40, 0.25% sodium deoxycholate, 1 mM phenylmethylsulfonyl fluoride [PMSF], 1× Roche complete mini-protease inhibitor cocktail) on ice, followed by centrifugation. Cell lysates were resolved by SDS-PAGE, transferred to nitrocellulose membranes, and subjected to immunoblotting. For coimmunoprecipitations (co-IPs), lysates were diluted 1:1 in RIPA buffer and precleared with protein A agarose beads (Roche Applied Science) for 60 min at 4°C. Precleared lysates were further incubated at 4°C overnight with the indicated antibodies (1 to 3 μl) and protein A agarose. Immunoprecipitates were washed three times with RIPA buffer followed by the addition of 20 μl 2× Laemmli sample buffer (LSB) to elute bound proteins. An additional wash with RIPA buffer supplemented with 1 M urea was performed for ubiquitination assays.

ELISAs. HTLV-1 p19 enzyme-linked immunosorbent assays (ELISAs) were performed according to the manufacturer's instructions using supernatants from MT-2 and 293T cells transfected with HTLV-1 proviral clones. Values were expressed in mean pg/ml ± standard errors of the means (SEM) as calculated from a standard curve derived from recombinant p19 provided in the HTLV-1 p19 ELISA kit (ZeptoMetrix).

Confocal microscopy. 293T and C8166 cells were cultured overnight on glass coverslips coated with poly-L-lysine in 12-well plates. Cells were fixed with 1% paraformaldehyde for 10 min and permeabilized with 0.2% Triton X-100 for 10 min. The fixed cells were then incubated with SuperBlock buffer (Thermo Scientific) for 45 min followed by staining with mouse anti-Tax and either anti-lamin B2, anti-CD25, anti-HSP90, or anti-20S proteasome rabbit antibodies. In some experiments, Alexa Fluor 647 Phalloidin (Life Technologies) was used to stain the actin cytoskeleton. Finally, coverslips were incubated with Alexa Fluor 555-conjugated donkey anti-mouse IgG, Alexa Fluor 488-conjugated donkey anti-rabbit IgG (Life Technologies,), and DAPI to stain nuclei. Images were obtained using a Nikon C1si confocal microscope.

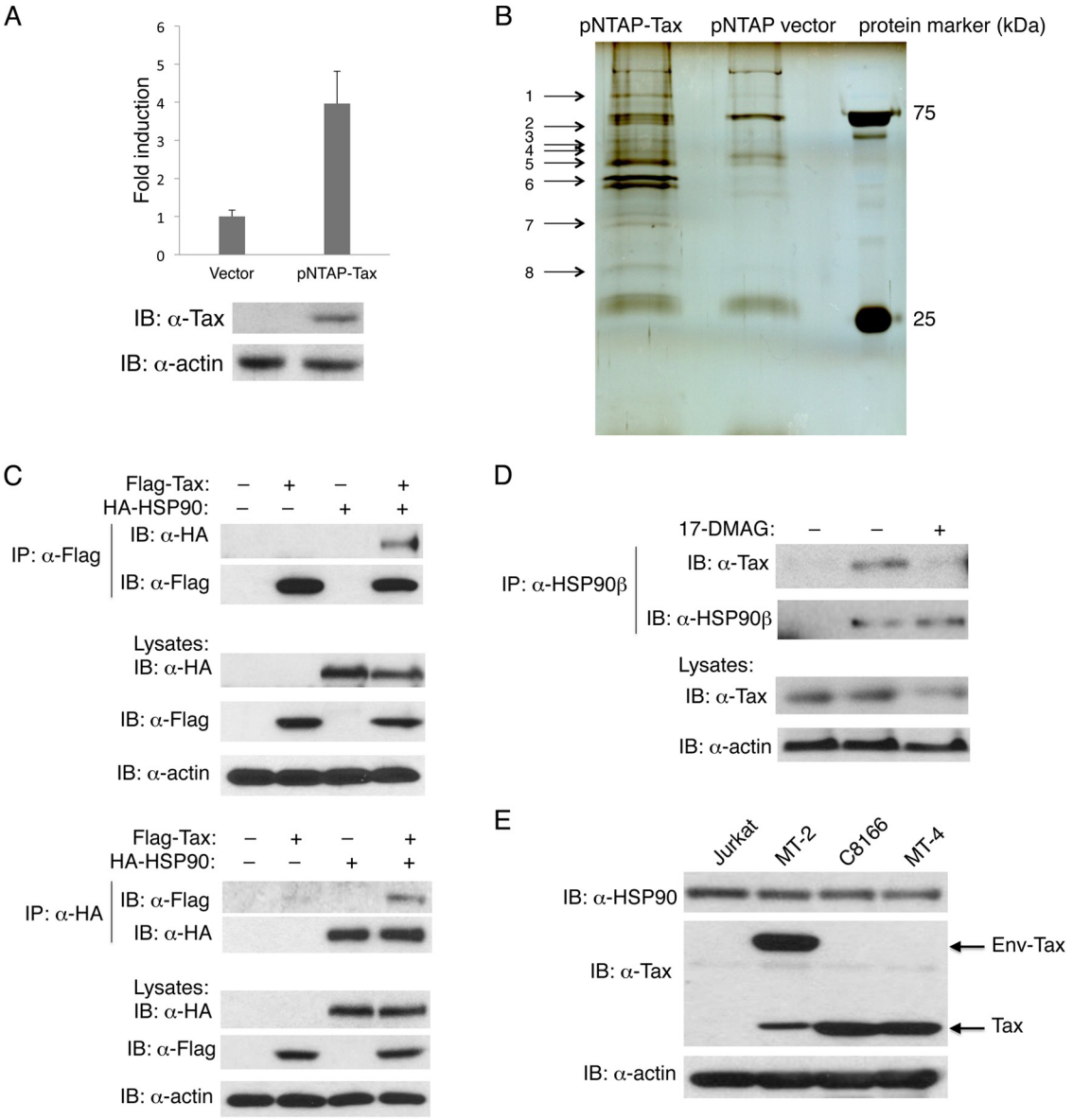
A
Fold induction
Vector
pNTAP-Tax
IB: α-Tax
IB: α-actin
B
pNTAP-Tax
pNTAP vector
protein marker (kDa)
75
25
C
Flag-Tax:
HA-HSP90:
IP: α-Flag
IB: α-HA
IB: α-Flag
Lysates:
IB: α-HA
IB: α-Flag
IB: α-actin
IP: α-HA
D
17-DMAG:
IP: α-HSP90β
IB: α-Tax
IB: α-HSP90β
Lysates:
E
Jurkat
MT-2
C8166
MT-4
IB: α-HSP90
IB: α-Tax
Env-Tax
Tax
IB: α-actin
F
Tax
HSP90
Phalloidin
DAPI
Tax+HSP90+DAPI
DAPI+Phalloidin
G
Merge

RT-PCR and qRT-PCR. Cells were treated with 0.5 μM 17-DMAG, and RNA was isolated using the RNeasy minikit (Qiagen). RNA was converted to cDNA using the First Strand cDNA synthesis kit for reverse transcription (RT)-PCR (avian myeloblastosis virus [AMV]; Roche Applied Science). Quantitative real-time PCR (qRT-PCR) was performed with an Applied Biosystems 7500 Real-Time PCR system using RT^2 SYBR green qPCR Mastermix (Qiagen). Gene expression was normalized to the internal control 18S rRNA. RT-PCR was performed using platinum PCR SuperMix (Life Technologies) to detect HTLV-1 p19 mRNA. GAPDH was used as an internal control. The following primers were used for qRT-PCR and RT-PCR: Tax forward primer, 5′-ATACCCAGTCTACGTGTTTGGAG-3′; Tax reverse primer, 5′-CCGATAACGCGTCCATCGATG-3′; HTLV-1 p19 forward primer, 5′-CACCCCTTTCCCTTTCATTCACGA-3′; HTLV-1 p19, reverse primer, 5′-CCGGCCGGGGTATCCTTTT-3′.

Subcellular fractionation. Subcellular fractionation was performed as described previously (32, 33). Cytoplasmic, soluble, and insoluble nuclear extracts were prepared using hypotonic buffer (20 mM HEPES, pH 8.0, 10 mM KCl, 1 mM $MgCl_2$, 0.1% [vol/vol] Triton X-100, and 20% [vol/vol] glycerol), hypertonic buffer (20 mM HEPES, pH 8.0, 1 mM EDTA, 20% [vol/vol] glycerol, 0.1% [vol/vol] Triton X-100, and 400 mM NaCl), and insoluble buffer (20 mM Tris, pH 8.0, 150 mM NaCl, 1% [wt/vol] SDS, 1% [vol/vol] NP-40, and 10 mM iodoacetamide), respectively. For the nuclear matrix, the cells were lysed sequentially to remove the cytoplasm, nucleoplasm, and chromatin using the hypotonic buffer, hypertonic buffer, and digestion buffer (200 U/ml DNase I, 100 mM NaCl, 300 mM sucrose, 10 mM PIPES [piperazine-*N*,*N*′-bis(2-ethanesulfonic acid)], pH 6.8, 3 mM $MgCl_2$, 0.5% Triton X-100, 1 mM PMSF, 1 μg/ml leupeptin, and 1 μg/ml pepstatin A), respectively. After 3 washes with the high-salt buffer (2 M NaCl, 300 mM sucrose, 10 mM PIPES, pH 6.8, 3 mM $MgCl_2$, 0.5% Triton X-100, 1 mM PMSF, 1 μg/ml leupeptin, and 1 μg/ml pepstatin A), the remaining pellet consisted of the nuclear matrix fraction. The purity of the obtained fractions was confirmed by examining LDH (cytoplasm), Sp1 (soluble nuclear fraction), or lamin B2 (nuclear matrix). All lysis buffers were supplemented with 1 mM PMSF and a protease inhibitor cocktail (Roche Applied Science).

Knockdown of HSP90 and Tax with lentiviral shRNA. Two lentiviral Mission short hairpin RNA (shRNA) clones targeting HSP90 beta were obtained from Sigma. HEK 293T cells were transfected with the lentiviral shRNA-targeting vectors pAX packaging plasmid and vesicular stomatitis virus glycoprotein (VSV-G). After 48 h, the supernatants were collected and centrifuged at 25,000 rpm for 2 h at 4°C. The supernatants were removed, and the pellets were resuspended in ice-cold phosphate-buffered saline (PBS). Viral stocks were used to infect C8166 and MT-2 cells and selected with puromycin (1 μg/ml for C8166 cells and 2 μg/ml for MT-2 cells). To suppress Tax expression in C8166 cells, the Tax sequence 5′-GCTTAGAGCCTCCCAGTGAAA-3′ was selected for shRNA targeting. The PYNC352 lentiviral vector was used to express control or Tax shRNA. Lentiviruses expressing Tax or control scrambled shRNA were generated as described above. C8166 cells were infected with lentiviruses and selected with puromycin (1 μg/ml) 48 h after infection.

Cell viability and proliferation assays. Cell viability was determined using the CellTiter-Glo luminescent cell viability assay (Promega), which quantitates ATP as a measure of metabolically active cells. Cells were placed in 96-well plates and treated with 17-DMAG. A total of 100 μl of suspended cells and 100 μl of CellTiter-Glo solution were mixed and incubated at room temperature for 10 min, and the luminescence was quantified with a GloMax96 microplate luminometer (Promega).

Statistical analysis. Data are expressed as mean fold increase ± standard deviation relative to the control from a representative experiment performed 3 times in triplicate. In the figures, an asterisk (*) indicates a P value of <0.05 as determined by Student's t test.

RESULTS

HTLV-1 Tax interacts with HSP90. To gain more insight into the molecular mechanisms of Tax regulation and oncogenesis, we sought to identify new Tax-binding proteins. The InterPlay Mammalian tandem affinity purification (TAP) system was used to purify Tax and its interacting proteins, which were then subjected to mass spectrometry (LC-MS/MS) analysis to identify protein complex components. Tax was cloned into the pNTAP expression vector in frame with the streptavidin-binding peptide (SBP) and calmodulin-binding peptide (CBP) affinity tags located upstream of Tax. Tax fused with the SBP and CBP tags was still able to activate NF-κB (Fig. 1A). 293T cells were transiently transfected with pNTAP empty vector or pNTAP-Tax, and two consecutive purification steps were conducted for the isolation of Tax and associated protein complexes. Purified proteins were resolved by SDS-PAGE, followed by silver staining, and the indicated pNTAP-Tax-specific bands (1 to 8) were excised from the gel and subjected to mass spectrometry (Fig. 1B). Known Tax-binding proteins, including protein phosphatase 2A (PP2A) (34), were identified in this screen (Table 1). HSP90 beta (a total of 25 peptides) was also identified as a novel Tax-binding protein (Table 1) and was selected for further study.

To validate the interaction between Tax and HSP90, co-IPs were performed with epitope-tagged Tax and HSP90 plasmids transfected into 293T cells. As shown in Fig. 1C (top), HSP90 interacted with immunoprecipitated Tax when both proteins were overexpressed. The reciprocal IP in which HSP90 was immunoprecipitated also confirmed Tax and HSP90 interaction (Fig. 1C, bottom). To determine if endogenous Tax and HSP90 proteins formed a complex, we next examined the interactions between Tax and HSP90 in the HTLV-1-transformed T-cell line MT-2. Indeed, Tax interacted with HSP90 in MT-2 cells, and this interaction was disrupted by treatment with the HSP90 inhibitor 17-DMAG (Fig. 1D). We next compared by Western blotting the relative levels of endogenous HSP90 in Jurkat T cells with those of HTLV-1-transformed cell lines MT-2, C8166, and MT-4. These results indicated that HSP90 levels were similar in these four cell lines (Fig. 1E). To determine where in the cells Tax and HSP90 interacted, we next performed confocal microscopy with 293T

FIG 1 HSP90 interacts with HTLV-1 Tax. (A) 293T cells were transfected with pNTAP-Tax, pRL-tk, and NF-κB-luciferase plasmids. After 24 h, cells were lysed and subjected to a dual-luciferase assay. Lysates were subjected to immunoblotting with anti-Tax and antiactin. (B) 293T cells were transiently transfected with pNTAP-Tax or pNTAP empty vector. Tandem affinity purification was performed using sequential purification steps with streptavidin and calmodulin resin. The purified Tax and associated protein complexes were resolved by SDS-PAGE and silver staining. The bands indicated by the arrows were excised and subjected to LC-MS/MS analysis. (C) 293T cells were transfected with Flag-Tax and HA-HSP90 plasmids as indicated. After 24 h, cell lysates were immunoprecipitated with Flag antibody and immunoblotting was performed with anti-HA and anti-Flag (top panel). The reciprocal IP was also performed with HA antibody and immunoblotting with anti-Flag (bottom panel). Lysates were subjected to immunoblotting with anti-HA, anti-Flag, and antiactin. (D) MT-2 cells were treated with the HSP90 inhibitor 17-DMAG (0.5 μM) for 2 h as indicated. Cell lysates were immunoprecipitated with HSP90 beta antibody, and immunoblotting was performed with anti-Tax and anti-HSP90 beta. (E) Jurkat, MT-2, C8166, and MT-4 cells were lysed and subjected to immunoblotting with anti-HSP90, anti-Tax, and antiactin. (F) 293T cells were transfected with GFP-Tax and HA-HSP90 plasmids. After 24 h, cells were stained with DAPI, phalloidin, and anti-HA and subjected to confocal microscopy. (G) C8166 cells were stained with DAPI, anti-Tax, and anti-HSP90 and subjected to confocal microscopy.

TABLE 1 Tax-interacting proteins identified by MS/MS

Band no.	Protein	No. of unique peptides	Molecular mass (kDa)
1	Propionyl-coenzyme A carboxylase alpha chain, mitochondrial isoform A precursor	35	80
1	Heat shock protein HSP90-beta	25	83
1	Methylcrotonoyl-coenzyme A carboxylase subunit alpha, mitochondrial precursor	20	80
1	Heat shock protein HSP90-alpha isoform 1	7	98
1	Trifunctional enzyme subunit alpha, mitochondrial precursor	4	83
2	Heat shock cognate 71-kDa protein isoform 1	29	71
2	Heat shock 70-kDa protein 1A/1B	25	70
2	Dystrobrevin beta isoform 1	7	71
2	SAM domain- and HD domain-containing protein 1	4	72
2	Probable ATP-dependent RNA helicase DDX17 isoform 3	4	80
3	60-kDa heat shock protein, mitochondrial	29	61
3	Beta-2-syntrophin	27	58
3	T-complex protein 1 subunit alpha isoform A	11	60
3	Serine/threonine-protein phosphatase 2A 65-kDa regulatory subunit A alpha isoform	6	65
3	T-complex protein 1 subunit epsilon	4	60
3	MAGUK p55 subfamily member 2	2	62
4	Beta-2-syntrophin	27	58
4	Propionyl-coenzyme A carboxylase beta chain, mitochondrial isoform 1	27	58
4	Phenylalanine-tRNA ligase alpha subunit	8	58
5	ATP synthase subunit alpha, mitochondrial isoform A precursor	25	60
5	Tubulin beta chain	22	50
5	Propionyl-coenzyme A carboxylase beta chain, mitochondrial isoform 1	18	58
5	Tubulin alpha-1B chain	18	50
5	Heterogeneous nuclear ribonucleoprotein H	9	49
5	Tubulin beta-6 chain	5	50
5	Tubulin beta-4b chain	4	50
5	Aldehyde dehydrogenase X, mitochondrial precursor	4	57
6	Tubulin alpha-1b chain	5	50
6	Elongation factor 1-alpha 1	4	50
6	Elongation factor Tu, mitochondrial precursor	3	50
6	DnaJ homolog subfamily A member 2	3	46
6	DnaJ homolog subfamily A member 1	2	45
6	Heterogeneous nuclear ribonucleoprotein F	2	46
7	Mitochondrial import inner membrane translocase subunit TIM50	5	50
7	Replication factor C subunit 3 isoform 2	2	35
7	Protein transport protein Sec61 subunit alpha isoform 1	2	52
7	Nucleophosmin isoform 1	2	33
7	Galactokinase	2	42
8	Phosphate carrier protein, mitochondrial isoform B precursor	8	40
8	ATP synthase subunit gamma, mitochondrial isoform L (liver) precursor	6	33
8	40S ribosomal protein S3	5	27
8	40S ribosomal protein S3a	4	30
8	WD repeat-containing protein 82	4	35
8	Serine/threonine-protein phosphatase PGAM5, mitochondrial isoform 1	4	32
8	Pyrroline-5-carboxylate reductase 1, mitochondrial isoform 1	3	33
8	Guanine nucleotide-binding protein subunit beta-2-like 1	3	35
8	Sideroflexin-1	2	36

cells transfected with GFP-Tax and HA-HSP90. HSP90 is known to be predominantly a cytoplasmic protein (35), whereas Tax shuttles between the nucleus and cytoplasm and can be found in both compartments at steady state (36, 37). As expected, HSP90 was distributed mainly in the cytoplasm and GFP-Tax exhibited punctate staining in both the nucleus and the cytoplasm (Fig. 1F). Fractions of Tax and HSP90 were found to colocalize in the cytoplasm (Fig. 1F). Next, we examined by confocal microscopy the

FIG 2 Inhibition of HSP90 promotes Tax degradation. (A) C8166, MT-2, and MT-4 cells were treated with 17-DMAG as indicated, and cell lysates were subjected to immunoblotting with the indicated antibodies. (B) C8166 cells were treated with 17-DMAG (0.5 μM) for 4 h, stained with DAPI, anti-Tax (red), and anti-GM-130 (green), and subjected to confocal microscopy. The bottom right panel shows merged images. (C) C8166 cells were treated with 17-DMAG (0.5 μM), and RNA was extracted for qRT-PCR analysis with Tax primers. (D) C8166 and MT-2 cells were infected with lentiviruses expressing two distinct HSP90 shRNAs and selected with puromycin. Cell lysates were subjected to immunoblotting with anti-Tax, anti-HSP90, and antiactin. (E) 293T cells were transfected with Tax, Tax M22, and Tax M47 plasmids. After 24 h, the cells were treated with 17-DMAG (0.5 μM) as indicated and cell lysates were subjected to immunoblotting with anti-Tax and antiactin. (F) 293T cells were transfected with HA-HSP90, Flag-Tax, Tax M22, and Tax M47 plasmids. After 24 h, cell lysates were immunoprecipitated with anti-Tax, and immunoblotting was performed with anti-HA and anti-Tax. Lysates were subjected to immunoblotting with anti-HA, anti-Tax, and antiactin.

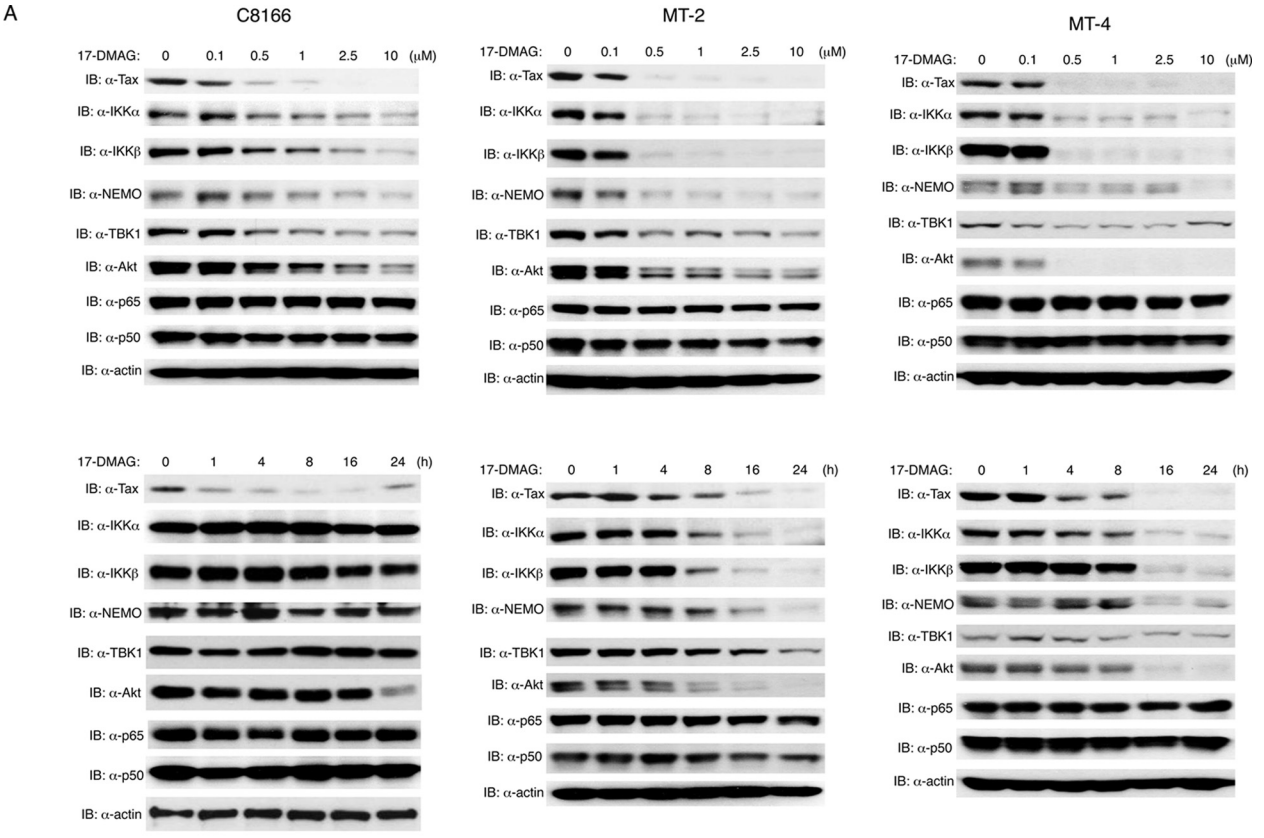
A
C8166
MT-2
MT-4
17-DMAG: 0 0.1 0.5 1 2.5 10 (μM)
17-DMAG: 0 1 4 8 16 24 (h)
IB: α-Tax
IB: α-IKKα
IB: α-IKKβ
IB: α-NEMO
IB: α-TBK1
IB: α-Akt
IB: α-p65
IB: α-p50
IB: α-actin

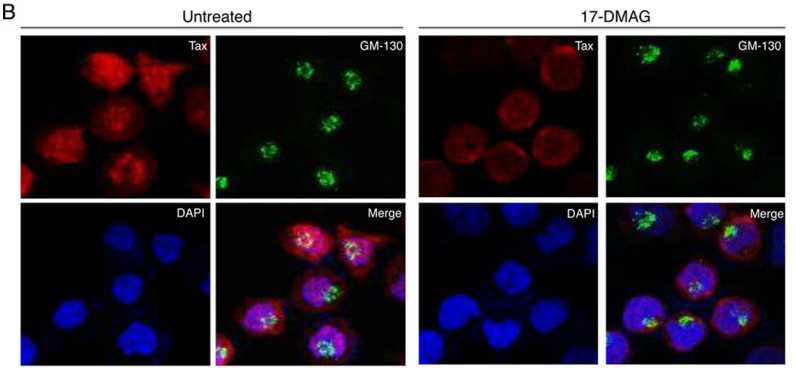
B
Untreated
17-DMAG
Tax
GM-130
DAPI
Merge

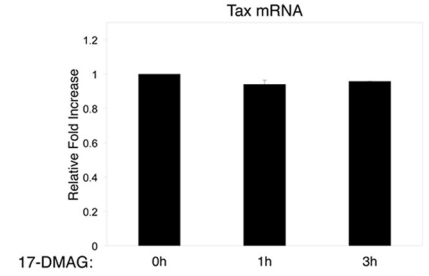
C
Tax mRNA
Relative Fold Increase
1.2
1
0.8
0.6
0.4
0.2
0
17-DMAG:
0h
1h
3h

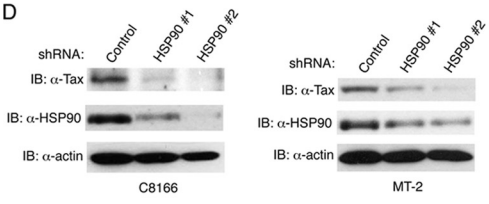
D
shRNA: Control HSP90 #1 HSP90 #2
IB: α-Tax
IB: α-HSP90
IB: α-actin
C8166
MT-2

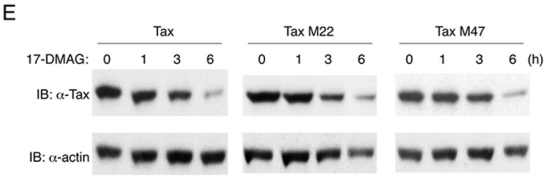
E
Tax
Tax M22
Tax M47
17-DMAG: 0 1 3 6 (h)
IB: α-Tax
IB: α-actin

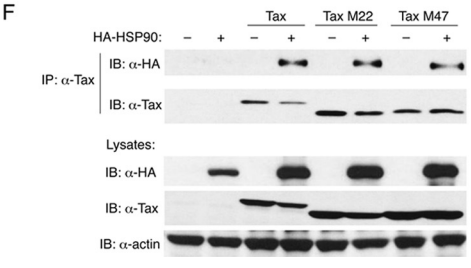
F
Tax
Tax M22
Tax M47
HA-HSP90: − + − + − + − +
IP: α-Tax
IB: α-HA
IB: α-Tax
Lysates:
IB: α-HA
IB: α-Tax
IB: α-actin

localization of endogenous Tax and HSP90 proteins in the HTLV-1-transformed cell line C8166. Tax strongly colocalized with HSP90 in C8166 cells, both in the cytoplasm and in the nucleus (Fig. 1G). HSP90 is known to translocate to the nucleus in response to stress signals or interaction with viral proteins (38–40). Taken together, HSP90 interacts with and colocalizes with Tax, and this interaction is disrupted by HSP90 inhibitors.

HSP90 inhibitors induce Tax degradation. HSP90 inhibitors such as geldanamycin and 17-DMAG potently induce the degradation of HSP90 client proteins (40, 41). A total of three HTLV-1-transformed cell lines, C8166, MT-2, and MT-4, were treated with different concentrations of 17-DMAG for 24 h. As shown in Fig. 2A (upper panel), 17-DMAG induced a substantial loss of Tax protein in all three cell lines. Known HSP90 client proteins IKKα, IKKβ, NEMO, AKT, and TBK1 (42–46) were also examined by immunoblotting as positive controls. MT-2 and MT-4 cells exhibited greater sensitivity to IKKα, IKKβ, NEMO, and AKT degradation than did C8166 cells (Fig. 2A). TBK1 degradation was not strongly induced by 17-DMAG in any of the cell lines (Fig. 2A). Levels of p65 and p50 were examined as negative controls, and as expected, 17-DMAG did not promote the degradation of these proteins (Fig. 2A). Based on these experiments, 0.5 μm 17-DMAG was found to be the lowest concentration that triggers Tax degradation; hence, this concentration was used in subsequent studies. We next stimulated the same three cell lines with 0.5 μM 17-DMAG to examine the kinetics of Tax degradation by immunoblotting. Tax was rapidly degraded (in 1 to 4 h) by 17-DMAG in C8166 cells; however, Tax degradation occurred at later times (16 h) in MT-2 and MT-4 cells (Fig. 2A, lower panel). Confocal microscopy was next performed to examine the effect of 17-DMAG on Tax staining and localization. Tax is known to reside together with IKK within the *cis*-Golgi and colocalizes with GM-130 (a *cis*-Golgi matrix protein) (47). Tax is also present in the nucleus in punctate nuclear bodies, where it colocalizes with the SC-35 splicing factor (48). Tax staining, particularly nuclear Tax, was substantially diminished by 17-DMAG (Fig. 2B). To confirm that 17-DMAG was influencing Tax protein stability but not transcription, qRT-PCR was performed to examine the mRNA level of Tax in C8166 cells after 17-DMAG treatment. Although Tax protein was rapidly lost in response to 17-DMAG treatment in C8166 cells, Tax mRNA was not influenced by HSP90 inhibition (Fig. 2C).

To rule out the possibility of spurious off-target effects of 17-DMAG, we used lentiviral expressed shRNAs (a total of two) to suppress HSP90 beta expression in C8166 and MT-2 cells. HSP90 knockdown was confirmed by immunoblotting, and shRNA number 2 exhibited a greater capability of suppressing endogenous HSP90 expression in both C8166 and MT-2 cells (Fig. 2D). Knockdown of HSP90 correlated with diminished Tax protein in C8166 and MT-2 cells (Fig. 2D). Thus, HSP90 is clearly essential to prevent Tax degradation in HTLV-1-transformed cell lines.

We next examined the sensitivity of two well-characterized Tax mutants, Tax M22 and Tax M47, to 17-DMAG stimulation. The Tax M22 mutant contains alanine and serine residues substituted for threonine and leucine at positions 130 and 131 and is defective for NF-κB but retains CREB/ATF activation (49). The M47 mutant contains arginine and serine residues substituted for two leucines at positions 319 and 320 and is impaired in CREB/ATF but retains NF-κB activation (49). As shown in Fig. 2E, 17-DMAG induced the degradation of wild-type Tax, Tax M22, and Tax M47 with similar kinetics, suggesting that the Tax M22 and M47 mutants were also regulated by HSP90. Indeed, Tax M22 and M47 were found to interact with HSP90 by co-IP in 293T cells (Fig. 2F).

17-DMAG induces proteasomal degradation of Tax in the nuclear matrix. Experiments were next conducted to determine the mechanisms of Tax degradation upon HSP90 inhibition. Degradation of HSP90 client proteins occurs mainly via the ubiquitin-proteasome pathway but may also occur through other mechanisms such as autophagy (43). To explore the mechanisms of Tax degradation induced by 17-DMAG, C8166 cells were treated with 17-DMAG together with inhibitors of the proteasome (MG-132) or lysosome (bafilomycin A1 [BafA1] or ammonium chloride [NH_4Cl]), and Tax expression was examined by immunoblotting in both soluble and insoluble compartments. Inhibition of the proteasome partially blocked Tax degradation in the soluble compartment, whereas the lysosomal inhibitors had no effect (Fig. 3A). Interestingly, there was a substantial accumulation of Tax in the insoluble fraction after treatment with both 17-DMAG and MG-132 (Fig. 3A), suggesting that HSP90 inhibition results in Tax proteasomal degradation in an insoluble compartment.

Proteins targeted to the proteasome for degradation are usually conjugated with lysine 48 (K48)-linked polyubiquitin chains (50). Thus, we used a K48 linkage-specific polyubiquitin antibody to determine if Tax was conjugated with K48-linked polyubiquitin chains after C8166 cells were treated with 17-DMAG and MG-132. Treatment with 17-DMAG alone induced a modest increase in Tax K48-linked polyubiquitination (Fig. 3B), probably since most of the Tax protein was already degraded. However, when degradation of Tax was blocked with MG-132 pretreatment, K48-linked polyubiquitination of Tax was substantially increased (Fig. 3B). We also observed increased K63-linked polyubiquitination of Tax using a K63-Ub linkage-specific antibody after MG-132 treatment (Fig. 3C).

Tax was previously shown to be degraded by the proteasome in the nuclear matrix (33). The nuclear matrix consists of the nuclear framework found throughout the nucleoplasm and can be isolated biochemically from the insoluble nuclear fraction. To determine where Tax proteasomal degradation occurred in response to 17-DMAG, biochemical fractionation was used to isolate cytoplasmic, soluble nuclear, and nuclear matrix fractions of C8166 cells for immunoblotting experiments. LDH served as a marker for the cytoplasm, the transcription factor Sp1 was used as a marker for the soluble nuclear fraction, and the intermediate filament protein lamin B2, which lines the nucleoplasmic side of the inner nuclear membrane, was used as a marker for the nuclear matrix. As shown in Fig. 3D, 17-DMAG treatment triggered a loss of Tax protein in the cytoplasmic and nuclear fractions. However, 17-DMAG treatment combined with proteasome inhibition led to the accumulation of Tax exclusively within the insoluble nuclear matrix fraction (Fig. 3D). These data indicate that the nuclear matrix constitutes the main cellular location of Tax proteasomal degradation upon HSP90 inhibition.

To further examine Tax degradation by HSP90 inhibition, confocal microscopy was conducted to visualize Tax along with markers of the nuclear and plasma membranes. Since Tax predominantly accumulated in the insoluble fraction of cells treated with 17-DMAG and MG-132 (Fig. 3A), C8166 cells were stained with anti-Tax and either anti-lamin B2 (nuclear membrane marker) or anti-CD25 (plasma membrane marker) upon HSP90 inhibition. In untreated C8166 cells, Tax was localized in both cytoplasmic and nuclear compartments as expected (Fig. 3E). 17-

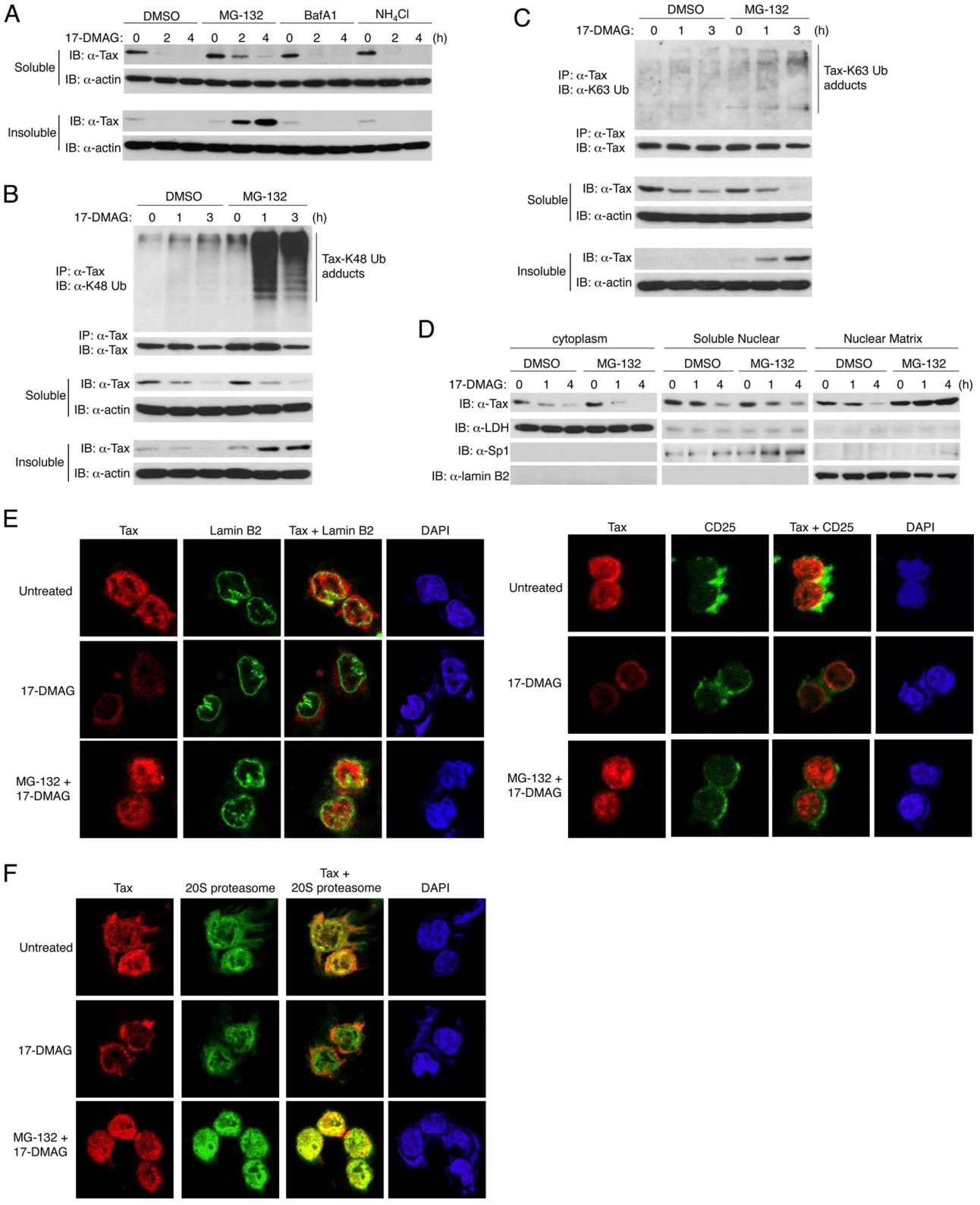

FIG 3 HSP90 inhibition induces Tax proteasomal degradation in the nuclear matrix. (A) C8166 cells were treated with 17-DMAG (0.5 μM) and either DMSO, MG-132 (20 μM), bafilomycin A1 (BafA1; 10 nM), or ammonium chloride (NH_4Cl; 20 μM) as indicated. Cells were lysed and partitioned into soluble and insoluble fractions and resolved by SDS-PAGE, and immunoblotting was performed with anti-Tax and antiactin. (B, C) C8166 cells were treated with 17-DMAG (0.5 μM) and MG-132 (20 μM) as indicated, soluble and insoluble cell lysates were immunoprecipitated with anti-Tax, and immunoblotting was performed with anti-K48 Ub (B), anti-K63 Ub (C), and anti-Tax. Lysates were also subjected to immunoblotting with anti-Tax and antiactin. (D) C8166 cells were treated with 17-DMAG (0.5 μM) and either DMSO or MG-132 (20 μM) as indicated, followed by fractionation into cytoplasmic, soluble nuclear, and nuclear matrix fractions. Immunoblotting was conducted with anti-Tax, anti-LDH, anti-Sp1, and anti-lamin B2. (E) C8166 cells were treated with 17-DMAG (0.5 μM) and MG-132 (20 μM) for 4 h as indicated and stained with DAPI, anti-Tax (red), anti-lamin B2 (left panel; green), and anti-CD25 (right panel; green). (F) C8166 cells were treated with 17-DMAG (0.5 μM) and MG-132 (20 μM) for 4 h as indicated and stained with DAPI, anti-Tax (red), and anti-20S proteasome (green).

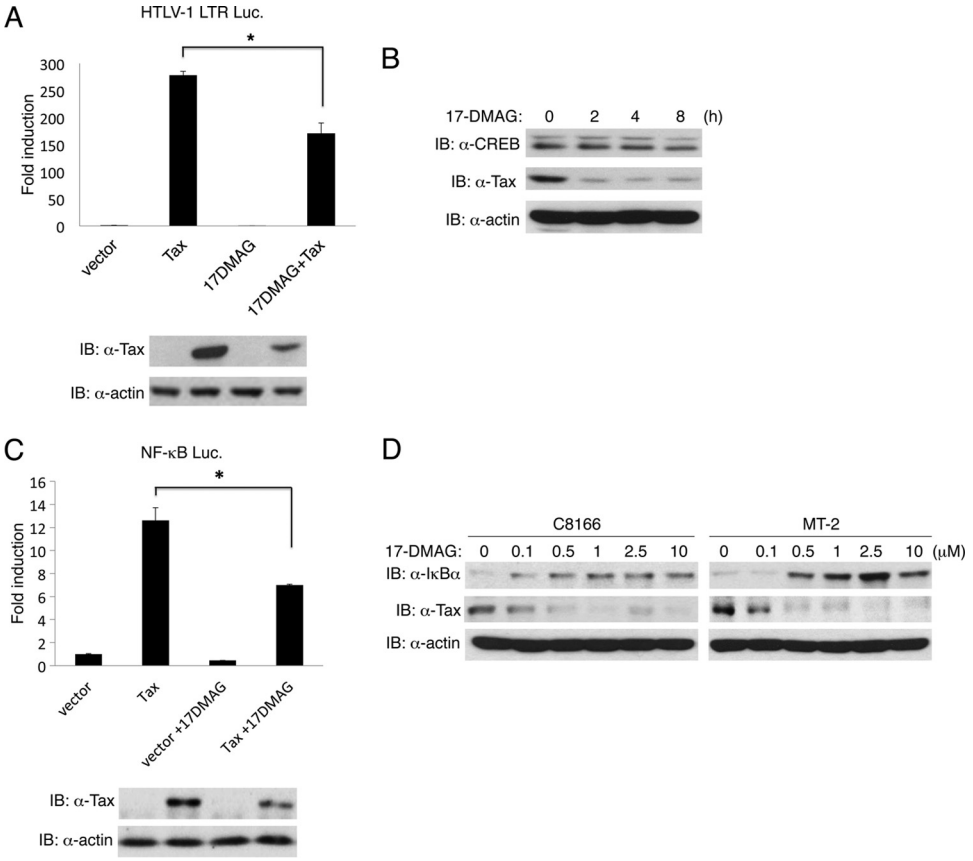

FIG 4 17-DMAG inhibits Tax-induced HTLV-1 LTR and NF-κB activation. (A) 293T cells were transfected with Flag-Tax, pRL-tk, and HTLV-1-LTR luciferase plasmids. After 24 h, the cells were treated with 17-DMAG (0.5 μM) for 16 h, and lysates were subjected to a dual-luciferase assay. Lysates were subjected to immunoblotting with anti-Tax and antiactin. (B) C8166 cells were treated with 17-DMAG (0.5 μM) for the indicated times, and cell lysates were subjected to immunoblotting with anti-CREB, anti-Tax, and antiactin. (C) 293T cells were transfected with Flag-Tax, pRL-tk, and NF-κB luciferase plasmids. After 24 h, the cells were treated with 17-DMAG (0.5 μM) for 16 h and lysates were subjected to a dual-luciferase assay. Lysates were subjected to immunoblotting with anti-Tax and antiactin. (D) C8166 cells and MT-2 cells were treated with the indicated concentrations of 17-DMAG for 24 h, and cell lysates were subjected to immunoblotting with anti-IκBα, anti-Tax, and antiactin. Error bars represent the standard deviations of triplicate samples (*, $P < 0.05$).

DMAG treatment dramatically depleted the nuclear fraction of Tax, leaving only a miniscule amount of cytoplasmic Tax (Fig. 3E). However, proteasome inhibition blocked Tax degradation by 17-DMAG and nuclear Tax was efficiently restored (Fig. 3E). Tax did not colocalize with CD25 (Fig. 3E), thus excluding the plasma membrane as a site for Tax degradation. Tax also did not appear to colocalize with lamin B2; therefore, although Tax degradation occurs within the nuclear matrix, it does not associate with lamin B2 (Fig. 3D).

A previous study has shown that Tax partially colocalizes with nuclear proteasomes (51). Therefore, we next stained C8166 cells with anti-Tax and anti-20S proteasome for confocal microscopy studies. In untreated C8166 cells, Tax partially colocalized with the 20S proteasome (Fig. 3F), consistent with a previous study (51). Upon 17-DMAG treatment, most of the Tax protein was depleted, and thus colocalization with the 20S proteasome was not observed (Fig. 3F). However, 17-DMAG together with MG-132 treatment resulted in a robust colocalization of Tax and 20S proteasome in the nucleus (Fig. 3F). It has been published that nuclear proteasomes are associated with the nuclear matrix, and most abundantly in the perinucleolar area (52). Since Tax strongly colocalized with the 20S proteasome in the nucleus after 17-DMAG and MG-132 treatment, it is likely that HSP90 opposes Tax K48-linked polyubiquitination and proteasomal degradation in the nuclear matrix.

17-DMAG inhibits Tax activation of NF-κB and the HTLV-1 LTR. We next determined if Tax function was influenced in response to HSP90 inhibition. Tax activation of the HTLV-1 LTR was examined by dual-luciferase assays. Tax expression induced a strong activation of the HTLV-1 LTR that was significantly blocked by 17-DMAG (Fig. 4A). 17-DMAG treatment was associated with less Tax expression in the lysates, suggesting that diminished Tax expression by HSP90 inhibition impaired LTR activation (Fig. 4A). Since Tax activates the LTR mainly through the CREB transcription factor, we next examined if 17-DMAG also destabilized CREB. However, CREB stability was not influenced by 17-DMAG in C8166 cells, although Tax was rapidly degraded by the treatment (Fig. 4B).

Next, we investigated the effect of HSP90 inhibition on Tax-mediated NF-κB activation. Tax activated an NF-κB luciferase reporter in 293T cells that was diminished by 17-DMAG (Fig. 4C). Again, 17-DMAG treatment was associated with lower Tax expression in the lysates (Fig. 4C), indicating that 17-DMAG does not directly suppress Tax *trans*-activation of promoters but rather

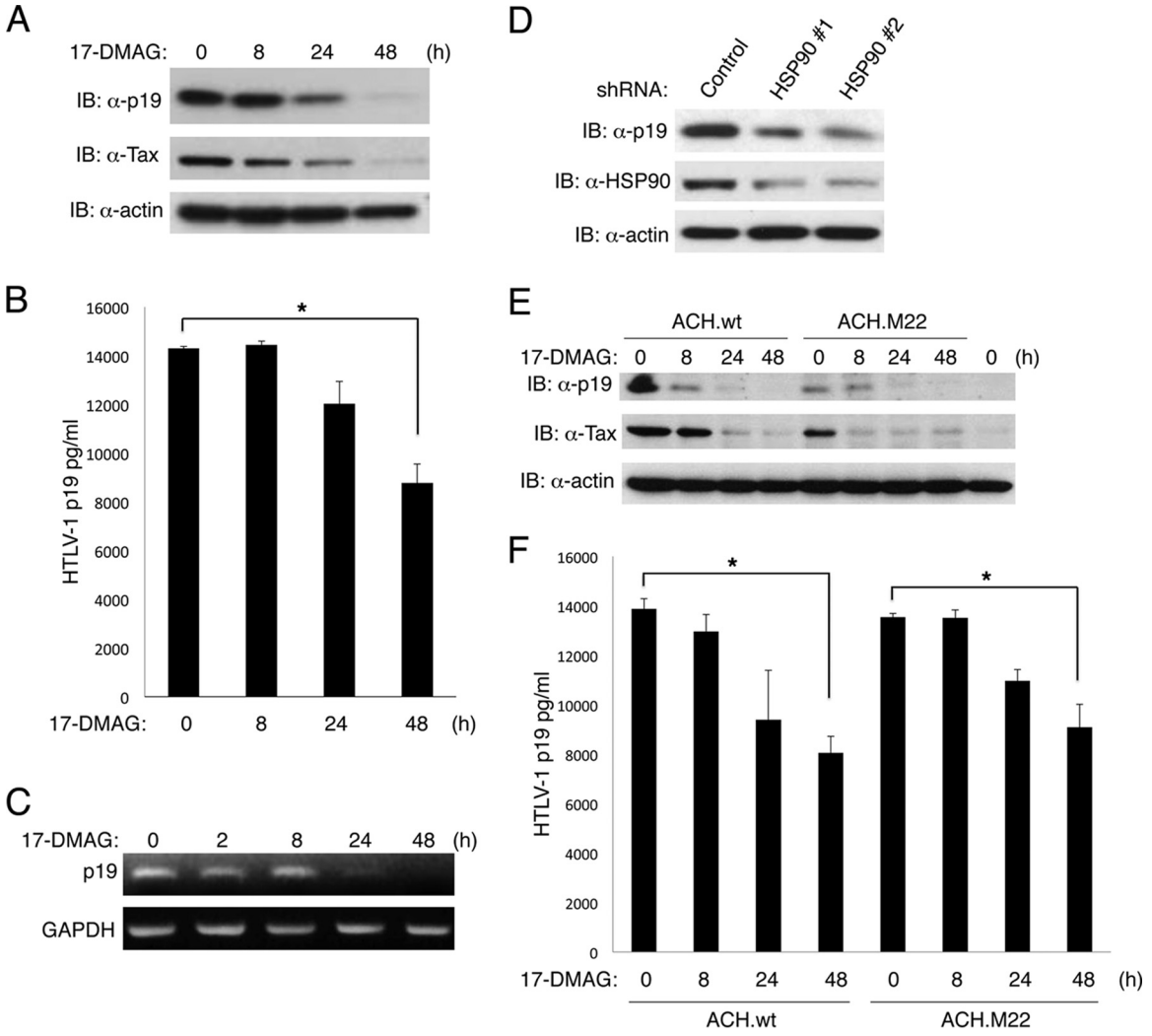

FIG 5 Inhibition of HSP90 blocks HTLV-1 replication. (A) MT-2 cells were treated with 17-DMAG (0.5 μM) for the indicated times, and cell lysates were subjected to immunoblotting with anti-HTLV-1 p19, anti-Tax, and antiactin. (B) Supernatants from MT-2 cells shown in panel A were subjected to HTLV-1 p19 ELISA. (C) MT-2 cells were treated with 17-DMAG (0.5 μM) for the indicated times, and RNA was extracted for RT-PCR with p19 and GAPDH primers. (D) MT-2 cells were infected with lentiviruses expressing control or HSP90 shRNAs. Immunoblotting was performed with anti-HTLV-1 p19, anti-HSP90, and antiactin. (E) 293T cells were transfected with HTLV-1 proviral clones ACH.wt or ACH.M22, and after 24 h cells were treated with 17-DMAG (0.5 μM) for the indicated times. Cell lysates were subjected to immunoblotting with anti-HTLV-1 p19, anti-Tax, and antiactin. (F) Supernatants of 293T cells from panel E were subjected to HTLV-1 p19 ELISA. Error bars represent the standard deviations of triplicate samples (*, $P < 0.05$).

reduces Tax expression. Since HSP90 inhibition also triggers IKK degradation (43), it is likely that the combined effects of Tax and IKK degradation suppressed Tax-mediated NF-κB activation. In HTLV-1-transformed cell lines, IKK is persistently activated, resulting in the constitutive phosphorylation and degradation of IκBα (53). HTLV-1-transformed cell lines C8166 and MT-2 cells were treated with different concentrations of 17-DMAG for 24 h, and IκBα was detected by immunoblotting. As shown in Fig. 4D, in the absence of 17-DMAG, IκBα was hardly detected, likely due to its persistent degradation. However, upon 17-DMAG treatment, Tax was degraded and IκBα levels were restored (Fig. 4D). Thus, HSP90 inhibition strongly blocks NF-κB activation in HTLV-1-transformed cell lines.

HSP90 inhibition suppresses HTLV-1 replication. We next examined the effects of HSP90 inhibition on HTLV-1 replication. MT-2 cells are commonly used as an efficient HTLV-1-producing cell line; therefore, we initially examined the effect of 17-DMAG on HTLV-1 replication in these cells. MT-2 cells were treated with 17-DMAG for different times, and immunoblotting was conducted to detect Tax and HTLV-1 p19, a major core viral protein encoded by the *gag* gene. 17-DMAG triggered a progressive decline of both Tax and p19 with complete loss of both proteins by 48 h of treatment (Fig. 5A). Supernatants from these cells were also subjected to an HTLV-1 p19 ELISA to quantitate the amount of cell-free HTLV-1. In agreement with the p19 immunoblotting results, there was significantly less cell-free HTLV-1 after 48 h of treatment with 17-DMAG (Fig. 5B). The diminished p19 and HTLV-1 levels in response to 17-DMAG treatment were likely due to decreased Tax expression and a block in viral LTR activation and transcription. To rule out direct effects of 17-DMAG on the p19 protein, RT-PCR was performed to detect p19 mRNA. After 24 h of 17-DMAG treatment, p19 mRNA sharply declined

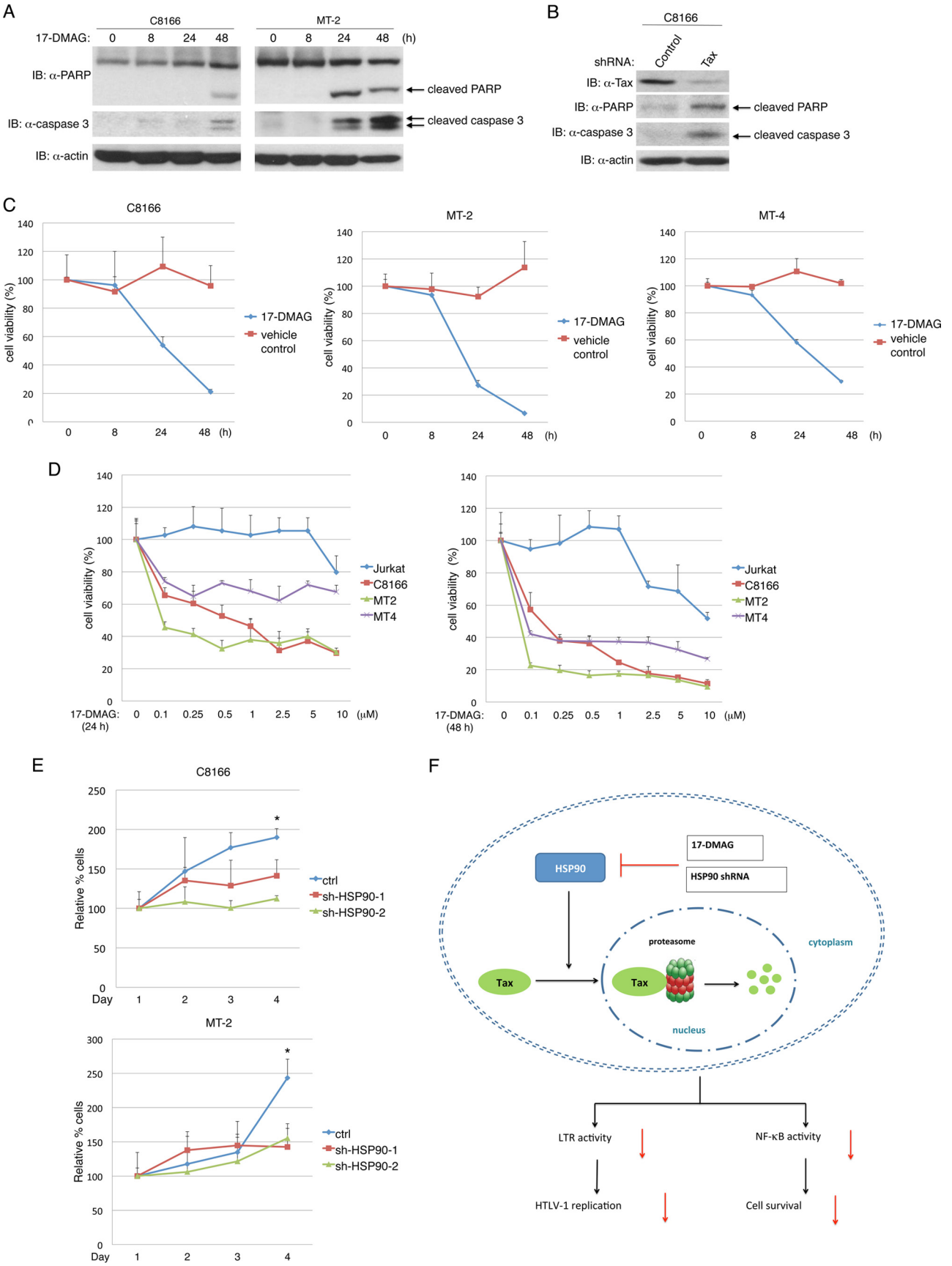
A
C8166
MT-2
17-DMAG: 0 8 24 48 0 8 24 48 (h)
IB: α-PARP
cleaved PARP
IB: α-caspase 3
cleaved caspase 3
IB: α-actin
B
C8166
shRNA: Control Tax
IB: α-Tax
IB: α-PARP
cleaved PARP
IB: α-caspase 3
cleaved caspase 3
IB: α-actin
C
C8166
MT-2
MT-4
cell viability (%)
17-DMAG
vehicle control
0 8 24 48 (h)
D
cell viability (%)
Jurkat
C8166
MT2
MT4
17-DMAG: 0 0.1 0.25 0.5 1 2.5 5 10 (μM)
(24 h)
(48 h)
E
C8166
MT-2
Relative % cells
Day
ctrl
sh-HSP90-1
sh-HSP90-2
F
HSP90
17-DMAG
HSP90 shRNA
proteasome
cytoplasm
Tax
nucleus
LTR activity
NF-κB activity
HTLV-1 replication
Cell survival

(Fig. 5C), indicating that the loss of p19 was due to transcriptional deficits owing to Tax degradation.

To rule out off-target effects of 17-DMAG, we also suppressed HSP90 expression in MT-2 cells using two distinct lentiviral HSP90 shRNAs. Both HSP90 shRNAs effectively inhibited HSP90 expression as shown by immunoblotting (Fig. 5D). Knockdown of HSP90 also resulted in decreased levels of p19 (Fig. 5D). These results reinforce the notion that HSP90 plays a critical role in supporting HTLV-1 replication.

The above-described experiments examined HTLV-1 replication in the context of a chronically infected HTLV-1-transformed cell line. We next examined HTLV-1 replication directed by a full-length HTLV-1 proviral clone. ACH.wt encodes wild-type Tax, whereas ACH.M22 encodes the Tax M22 mutant impaired in NF-κB activation (14). The HTLV-1 proviral clones were transfected in 293T cells that were subsequently treated with 17-DMAG for different times. Immunoblotting was conducted to examine levels of Tax and p19. Expression of p19 and Tax was evident after transfection of either ACH.wt or ACH.M22; however, 17-DMAG elicited strong downregulation of both Tax and p19 (Fig. 5E). Treatment with 17-DMAG for 48 h also resulted in a significant decrease in HTLV-1 p19 detected in the supernatants of these cells by ELISA (Fig. 5F). Taken together, these results suggest that inhibition of HSP90 by 17-DMAG or shRNA knockdown potently suppresses HTLV-1 replication.

17-DMAG induces apoptosis of HTLV-1-transformed cells. Tax and NF-κB are both essential for HTLV-1-induced oncogenesis and cell survival; therefore, we hypothesized that HSP90 inhibition would induce apoptotic cell death of HTLV-1-transformed cells. C8166 and MT-2 cells were treated with 17-DMAG for various times, and immunoblotting was conducted to detect cleaved forms of PARP and caspase 3, indicative of apoptotic cell death. Indeed, PARP and caspase 3 cleavage was detected after 48 h of treatment with 17-DMAG in C8166 cells, whereas PARP and caspase 3 cleavage occurred earlier in MT-2 cells (Fig. 6A). To confirm that C8166 cells were dependent on Tax expression for survival, we used a lentiviral shRNA to suppress Tax expression. Indeed, knockdown of Tax induced apoptosis of C8166 cells as revealed by cleaved PARP and caspase 3 (Fig. 6B). Trypan blue staining also confirmed a significant decrease in the viability of C8166 cells infected with lentiviruses expressing Tax but not control shRNA (data not shown). Therefore, it is likely that 17-DMAG-induced degradation of Tax contributes to cell death of HTLV-1-transformed cell lines.

We next examined the effect of 17-DMAG on the viability of the HTLV-1-transformed cell lines C8166, MT-2, and MT-4 using the CellTiter-Glo luminescent cell viability assay, which measures metabolically active cells by quantifying ATP levels. 17-DMAG promoted loss of cell viability for each of the tested cell lines beginning at 24 h and increasing at 48 h (Fig. 6C). MT-2 cells appeared to be more sensitive to 17-DMAG than MT-4 and C8166 cells (Fig. 6C).

We next examined the viability of C8166, MT-2, and MT-4 cells in response to different concentrations of 17-DMAG for 24 and 48 h. The HTLV-1-negative T-cell line Jurkat served as a negative control. As expected, Jurkat cells were largely insensitive to cell death induced by 17-DMAG. Treatment of Jurkat cells with 17-DMAG for 24 h led to a modest decrease of cell viability at the highest dose tested (10 μM), whereas all of the HTLV-1-transformed cells exhibited cell death with concentrations as low as 0.1 μM (Fig. 6D). After 17-DMAG treatment for 48 h, Jurkat cells exhibited greater sensitivity, and a modest loss of viability was observed with a concentration of 2.5 μM (Fig. 6D). Nevertheless, C8166, MT-2, and MT-4 cells exhibited a much greater sensitivity to 17-DMAG with nearly complete loss of viability at concentrations of 0.1 and 0.25 μM (Fig. 6D).

To determine if knockdown of HSP90 with shRNAs inhibited the proliferation of HTLV-1-transformed cells, we used C8166 and MT-2 cells infected with lentiviruses expressing two HSP90 shRNAs. Metabolically active cells were quantified every 24 h for 4 consecutive days as a measure of proliferation. Cells expressing control scrambled shRNA showed increased proliferation throughout the time course (Fig. 6E). However, the proliferation of C8166 and MT-2 cells with HSP90 knockdown was impaired compared to cells expressing control shRNA (Fig. 6E).

DISCUSSION

In this study, we have demonstrated that HTLV-1 Tax is a novel client protein of HSP90. Tax and HSP90 form a protein complex that is sensitive to the HSP90 inhibitor 17-DMAG. HSP90 serves a critical chaperone function for Tax and prevents its K48-linked polyubiquitination and proteasomal degradation in the nuclear matrix. Thus, inhibition of HSP90 with either shRNAs or 17-DMAG promotes Tax degradation. 17-DMAG is therefore a potent inhibitor of Tax and HTLV-1 replication and instigates apoptotic cell death of HTLV-1-transformed cells (Fig. 6F).

Accumulating evidence indicates that Tax dynamically shuttles between compartments in the cytoplasm and nucleus to carry out specific functions (28, 54). Tax interacts with the IKK complex within the *cis*-Golgi to persistently activate IKK and NF-κB signaling (47, 55), while Tax localized within nuclear bodies is involved in transcriptional regulation and may also regulate splicing and the DNA damage response (48, 56, 57). Posttranslational modifications of Tax including phosphorylation, ubiquitination, SUMOylation, and acetylation have all been shown to regulate Tax trafficking and/or function (58–60). A number of studies support the notion that Tax is a stable protein, but nevertheless, Tax proteasomal degradation occurs mainly in the nucleus, specifically in the nuclear matrix (28, 33, 51). The E3 ligase PDLIM2 targets Tax for K48-linked polyubiquitination and proteasomal

FIG 6 17-DMAG promotes apoptotic cell death of HTLV-1-transformed cell lines. (A) C8166 and MT-2 cells were treated with 17-DMAG (0.5 μM) for the indicated times, and the cell lysates were subjected to immunoblotting with anti-PARP, anti-caspase 3, and antiactin. (B) C8166 cells were infected with lentiviral Tax or control shRNA, and lysates were subjected to immunoblotting with anti-Tax, anti-PARP, anti-caspase 3, and antiactin. (C) C8166, MT-2, and MT-4 cells were treated with 17-DMAG (0.5 μM) or vehicle control for the indicated times. Cell viability was determined with CellTiter-Glo. (D) Jurkat, C8166, MT-2, and MT-4 cells were treated with the indicated concentrations of 17-DMAG for 24 h (left) and 48 h (right). Cell viability was determined with CellTiter-Glo. (E) C8166 and MT-2 cells infected with lentiviral HSP90 shRNAs were quantified for ATP levels at the indicated times using CellTiter-Glo. (F) Schematic model of HSP90 regulation of Tax. HSP90 inhibition by 17-DMAG or shRNA induces Tax proteasomal degradation, leading to suppressed LTR and NF-κB activation, HTLV-1 replication, and cell viability. Error bars represent the standard deviations of triplicate samples (*, $P < 0.05$).

degradation in the nuclear matrix (33). Our data are in agreement with these studies since 17-DMAG triggers Tax association with the 20S proteasome and degradation in the nuclear matrix. HSP90 may shuttle together with Tax and protect Tax from PDLIM2-mediated K48-linked polyubiquitination and degradation in the nucleus. It has been shown that arsenic trioxide and alpha interferon (IFN-α) synergize to promote Tax degradation, and this treatment regimen appears to be highly effective in a murine model of ATL (61, 62). It will be interesting to determine if arsenic/IFN-α influences Tax interaction with HSP90.

HSP90 is a highly conserved and ubiquitously expressed protein that plays an important role in the folding, conformational maturation, and trafficking of hundreds of client proteins (20). HSP90 is mainly a cytoplasmic protein; however, we have found that HSP90 is localized in both the cytoplasm and the nucleus of HTLV-1-transformed cells. This is likely due to HSP90 interaction with Tax, which shuttles between these compartments. Other viral proteins such as the herpes simplex virus 1 (HSV-1) polymerase and Kaposi's sarcoma herpesvirus (KSHV) LANA have also been shown to be localized in the nucleus together with HSP90 (39, 40). Indeed, there are an abundance of viral proteins that utilize HSP90 for proper folding, stabilization, and/or trafficking; thus, HSP90 inhibitors represent a potent new class of antiviral drugs with activity against a broad range of viruses, including influenza, hepatitis, and herpesviruses (63–65). Our results using chronically infected HTLV-1-producing cell lines and proviral clones indicate that HTLV-1 replication is also blocked by HSP90 inhibition.

In addition to inhibiting HTLV-1 replication, 17-DMAG also potently suppresses NF-κB activation and induces the apoptotic cell death of HTLV-1-transformed cell lines. These effects of 17-DMAG are likely due not solely to Tax degradation but also to the degradation of other HSP90 clients, including IKK and AKT and possibly others. Indeed, other studies have found that IKK is stabilized by HSP90 and that degradation of IKK by HSP90 inhibitors leads to loss of viability of ATL cells (45, 66). Nevertheless, we demonstrated that C8166 cells were critically dependent on Tax expression for survival, suggesting that 17-DMAG-induced Tax degradation clearly contributes to cell death in these cells. We found that HTLV-1-transformed cells were much more sensitive to 17-DMAG-induced cell death than were control Jurkat cells. However, expression of Tax in Jurkat cells did not sensitize the cells to 17-DMAG (data not shown). Heat shock proteins are frequently overexpressed in solid tumors and hematological malignancies, and these neoplasms exhibit increased dependence on heat shock proteins compared to normal untransformed cells due to stabilization of oncoproteins. This selective basis for targeting cancer cells has led to considerable interest in 17-DMAG and other HSP90 inhibitors as anticancer agents, and several clinical trials with HSP90 inhibitors are ongoing (67). Based on our results as well as previous studies, HSP90 inhibitors should be considered for clinical use for ATL and HAM/TSP patients. While our manuscript was under review, Ikebe et al. demonstrated an efficacious role of 17-DMAG in targeting Tax and improving survival in an ATL mouse model (68). Although Tax is often downregulated by genetic or epigenetic mechanisms in ATL leukemic cells (69), HSP90 inhibitors also target IKK, which plays a critical role in the survival of these malignant cells. HAM/TSP patients have high proviral loads and elevated Tax expression; thus, HSP90 inhibition would be expected to target Tax and reduce HTLV-1 replication and proviral loads.

In conclusion, a mass spectrometry screen has identified HSP90 as a novel Tax-interacting protein that protects Tax from proteasomal degradation in the nuclear matrix. Inhibition of HSP90 with shRNA or 17-DMAG destabilizes Tax and suppresses Tax-induced NF-κB and viral LTR activation, leading to reduced HTLV-1 replication and increased apoptotic cell death. This study provides new insight into the regulation of Tax stability by host factors and also suggests that HSP90 inhibitors may exert therapeutic benefits for ATL and HAM/TSP patients.

ACKNOWLEDGMENTS

We thank Bob Cole for performing mass spectrometry and analysis and the Johns Hopkins University School of Medicine Proteomic and Mass Spectrometry Core facility, Sidney Kimmel Comprehensive Cancer Center. We also acknowledge Lee Ratner for providing the HTLV-1 proviral clones, Young Choi for making Tax shRNA lentivirus, and Qinjie Zhou for generating HSP90 shRNA lentiviruses.

These studies were supported by NIH grants RO1CA135362 and PO1CA128115 and NCI center grant 2P30 CA006973.

The content of this article is solely the responsibility of the authors and does not necessarily represent the official views of the National Cancer Institute or the National Institutes of Health.

REFERENCES

1. **Poiesz BJ, Ruscetti FW, Gazdar AF, Bunn PA, Minna JD, Gallo RC.** 1980. Detection and isolation of type C retrovirus particles from fresh and cultured lymphocytes of a patient with cutaneous T-cell lymphoma. Proc. Natl. Acad. Sci. U. S. A. **77:**7415–7419.
2. **Iwanaga M, Watanabe T, Yamaguchi K.** 2012. Adult T-cell leukemia: a review of epidemiological evidence. Front. Microbiol. **3:**322. doi:10.3389/fmicb.2012.00322.
3. **Iwanaga M, Watanabe T, Utsunomiya A, Okayama A, Uchimaru K, Koh KR, Ogata M, Kikuchi H, Sagara Y, Uozumi K, Mochizuki M, Tsukasaki K, Saburi Y, Yamamura M, Tanaka J, Moriuchi Y, Hino S, Kamihira S, Yamaguchi K.** 2010. Human T-cell leukemia virus type I (HTLV-1) proviral load and disease progression in asymptomatic HTLV-1 carriers: a nationwide prospective study in Japan. Blood **116:**1211–1219.
4. **Grassmann R, Aboud M, Jeang KT.** 2005. Molecular mechanisms of cellular transformation by HTLV-1 Tax. Oncogene **24:**5976–5985.
5. **Kashanchi F, Brady JN.** 2005. Transcriptional and post-transcriptional gene regulation of HTLV-1. Oncogene **24:**5938–5951.
6. **Matsuoka M, Jeang KT.** 2007. Human T-cell leukaemia virus type 1 (HTLV-1) infectivity and cellular transformation. Nat. Rev. Cancer **7:**270–280.
7. **Sun SC, Yamaoka S.** 2005. Activation of NF-kappaB by HTLV-I and implications for cell transformation. Oncogene **24:**5952–5964.
8. **Hayden MS, Ghosh S.** 2012. NF-kappaB, the first quarter-century: remarkable progress and outstanding questions. Genes Dev. **26:**203–234.
9. **Sun SC, Ganchi PA, Ballard DW, Greene WC.** 1993. NF-kappa B controls expression of inhibitor I kappa B alpha: evidence for an inducible autoregulatory pathway. Science **259:**1912–1915.
10. **DiDonato JA, Hayakawa M, Rothwarf DM, Zandi E, Karin M.** 1997. A cytokine-responsive IkappaB kinase that activates the transcription factor NF-kappaB. Nature **388:**548–554.
11. **Karin M, Ben-Neriah Y.** 2000. Phosphorylation meets ubiquitination: the control of NF-[kappa]B activity. Annu. Rev. Immunol. **18:**621–663.
12. **Harhaj EW, Sun SC.** 1999. IKKgamma serves as a docking subunit of the IkappaB kinase (IKK) and mediates interaction of IKK with the human T-cell leukemia virus Tax protein. J. Biol. Chem. **274:**22911–22914.
13. **Jin DY, Giordano V, Kibler KV, Nakano H, Jeang KT.** 1999. Role of adapter function in oncoprotein-mediated activation of NF-kappaB. Human T-cell leukemia virus type I Tax interacts directly with IkappaB kinase gamma. J. Biol. Chem. **274:**17402–17405.
14. **Robek MD, Ratner L.** 1999. Immortalization of CD4(+) and CD8(+) T lymphocytes by human T-cell leukemia virus type 1 Tax mutants expressed in a functional molecular clone. J. Virol. **73:**4856–4865.
15. **Mori N, Fujii M, Ikeda S, Yamada Y, Tomonaga M, Ballard DW,**

Yamamoto N. 1999. Constitutive activation of NF-kappaB in primary adult T-cell leukemia cells. Blood **93:**2360–2368.
16. **Cann AJ, Rosenblatt JD, Wachsman W, Shah NP, Chen IS.** 1985. Identification of the gene responsible for human T-cell leukaemia virus transcriptional regulation. Nature **318:**571–574.
17. **Tie F, Adya N, Greene WC, Giam CZ.** 1996. Interaction of the human T-lymphotropic virus type 1 Tax dimer with CREB and the viral 21-base-pair repeat. J. Virol. **70:**8368–8374.
18. **Currer R, Van Duyne R, Jaworski E, Guendel I, Sampey G, Das R, Narayanan A, Kashanchi F.** 2012. HTLV tax: a fascinating multifunctional co-regulator of viral and cellular pathways. Front. Microbiol. **3:**406. doi:10.3389/fmicb.2012.00406.
19. **Taipale M, Jarosz DF, Lindquist S.** 2010. HSP90 at the hub of protein homeostasis: emerging mechanistic insights. Nat. Rev. Mol. Cell Biol. **11:** 515–528.
20. **Zhao R, Davey M, Hsu YC, Kaplanek P, Tong A, Parsons AB, Krogan N, Cagney G, Mai D, Greenblatt J, Boone C, Emili A, Houry WA.** 2005. Navigating the chaperone network: an integrative map of physical and genetic interactions mediated by the hsp90 chaperone. Cell **120:**715–727.
21. **Whitesell L, Lindquist SL.** 2005. HSP90 and the chaperoning of cancer. Nat. Rev. Cancer **5:**761–772.
22. **Ratzke C, Mickler M, Hellenkamp B, Buchner J, Hugel T.** 2010. Dynamics of heat shock protein 90 C-terminal dimerization is an important part of its conformational cycle. Proc. Natl. Acad. Sci. U. S. A. **107:**16101–16106.
23. **Panaretou B, Prodromou C, Roe SM, O'Brien R, Ladbury JE, Piper PW, Pearl LH.** 1998. ATP binding and hydrolysis are essential to the function of the Hsp90 molecular chaperone in vivo. EMBO J. **17:**4829–4836.
24. **Grenert JP, Sullivan WP, Fadden P, Haystead TA, Clark J, Mimnaugh E, Krutzsch H, Ochel HJ, Schulte TW, Sausville E, Neckers LM, Toft DO.** 1997. The amino-terminal domain of heat shock protein 90 (hsp90) that binds geldanamycin is an ATP/ADP switch domain that regulates hsp90 conformation. J. Biol. Chem. **272:**23843–23850.
25. **Neckers L, Workman P.** 2012. Hsp90 molecular chaperone inhibitors: are we there yet? Clin. Cancer Res. **18:**64–76.
26. **Charoenthongtrakul S, Zhou Q, Shembade N, Harhaj NS, Harhaj EW.** 2011. Human T cell leukemia virus type 1 Tax inhibits innate antiviral signaling via NF-kappaB-dependent induction of SOCS1. J. Virol. **85:** 6955–6962.
27. **Shembade N, Harhaj NS, Yamamoto M, Akira S, Harhaj EW.** 2007. The human T-cell leukemia virus type 1 Tax oncoprotein requires the ubiquitin-conjugating enzyme Ubc13 for NF-kappaB activation. J. Virol. **81:** 13735–13742.
28. **Lavorgna A, Harhaj EW.** 2012. An RNA interference screen identifies the Deubiquitinase STAMBPL1 as a critical regulator of human T-cell leukemia virus type 1 tax nuclear export and NF-kappaB activation. J. Virol. **86:**3357–3369.
29. **Turci M, Lodewick J, Righi P, Polania A, Romanelli MG, Bex F, Bertazzoni U.** 2009. HTLV-2B Tax oncoprotein is modified by ubiquitination and sumoylation and displays intracellular localization similar to its homologue HTLV-1 Tax. Virology **386:**6–11.
30. **Kimata JT, Wong FH, Wang JJ, Ratner L.** 1994. Construction and characterization of infectious human T-cell leukemia virus type 1 molecular clones. Virology **204:**656–664.
31. **Shevchenko A, Wilm M, Vorm O, Mann M.** 1996. Mass spectrometric sequencing of proteins silver-stained polyacrylamide gels. Anal. Chem. **68:**850–858.
32. **Tanaka T, Grusby MJ, Kaisho T.** 2007. PDLIM2-mediated termination of transcription factor NF-kappaB activation by intranuclear sequestration and degradation of the p65 subunit. Nat. Immunol. **8:**584–591.
33. **Yan P, Fu J, Qu Z, Li S, Tanaka T, Grusby MJ, Xiao G.** 2009. PDLIM2 suppresses human T-cell leukemia virus type I Tax-mediated tumorigenesis by targeting Tax into the nuclear matrix for proteasomal degradation. Blood **113:**4370–4380.
34. **Fu DX, Kuo YL, Liu BY, Jeang KT, Giam CZ.** 2003. Human T-lymphotropic virus type I tax activates I-kappa B kinase by inhibiting I-kappa B kinase-associated serine/threonine protein phosphatase 2A. J. Biol. Chem. **278:**1487–1493.
35. **Kang KI, Devin J, Cadepond F, Jibard N, Guiochon-Mantel A, Baulieu EE, Catelli MG.** 1994. In vivo functional protein-protein interaction: nuclear targeted hsp90 shifts cytoplasmic steroid receptor mutants into the nucleus. Proc. Natl. Acad. Sci. U. S. A. **91:**340–344.
36. **Alefantis T, Barmak K, Harhaj EW, Grant C, Wigdahl B.** 2003. Characterization of a nuclear export signal within the human T cell leukemia virus type I transactivator protein Tax. J. Biol. Chem. **278:**21814–21822.
37. **Burton M, Upadhyaya CD, Maier B, Hope TJ, Semmes OJ.** 2000. Human T-cell leukemia virus type 1 Tax shuttles between functionally discrete subcellular targets. J. Virol. **74:**2351–2364.
38. **Akner G, Mossberg K, Sundqvist KG, Gustafsson JA, Wikstrom AC.** 1992. Evidence for reversible, non-microtubule and non-microfilament-dependent nuclear translocation of hsp90 after heat shock in human fibroblasts. Eur. J. Cell Biol. **58:**356–364.
39. **Burch AD, Weller SK.** 2005. Herpes simplex virus type 1 DNA polymerase requires the mammalian chaperone hsp90 for proper localization to the nucleus. J. Virol. **79:**10740–10749.
40. **Chen W, Sin SH, Wen KW, Damania B, Dittmer DP.** 2012. Hsp90 inhibitors are efficacious against Kaposi Sarcoma by enhancing the degradation of the essential viral gene LANA, of the viral co-receptor EphA2 as well as other client proteins. PLoS Pathog. **8:**e1003048. doi:10.1371/journal.ppat.1003048.
41. **Pozo FM, Oda T, Sekimoto T, Murakumo Y, Masutani C, Hanaoka F, Yamashita T.** 2011. Molecular chaperone Hsp90 regulates REV1-mediated mutagenesis. Mol. Cell. Biol. **31:**3396–3409.
42. **Chen G, Cao P, Goeddel DV.** 2002. TNF-induced recruitment and activation of the IKK complex require Cdc37 and Hsp90. Mol. Cell **9:**401–410.
43. **Qing G, Yan P, Xiao G.** 2006. Hsp90 inhibition results in autophagy-mediated proteasome-independent degradation of IkappaB kinase (IKK). Cell Res. **16:**895–901.
44. **Hertlein E, Wagner AJ, Jones J, Lin TS, Maddocks KJ, Towns WH, III, Goettl VM, Zhang X, Jarjoura D, Raymond CA, West DA, Croce CM, Byrd JC, Johnson AJ.** 2010. 17-DMAG targets the nuclear factor-kappaB family of proteins to induce apoptosis in chronic lymphocytic leukemia: clinical implications of HSP90 inhibition. Blood **116:**45–53.
45. **Kurashina R, Ohyashiki JH, Kobayashi C, Hamamura R, Zhang Y, Hirano T, Ohyashiki K.** 2009. Anti-proliferative activity of heat shock protein (Hsp) 90 inhibitors via beta-catenin/TCF7L2 pathway in adult T cell leukemia cells. Cancer Lett. **284:**62–70.
46. **Yang K, Shi H, Qi R, Sun S, Tang Y, Zhang B, Wang C.** 2006. Hsp90 regulates activation of interferon regulatory factor 3 and TBK-1 stabilization in Sendai virus-infected cells. Mol. Biol. Cell **17:**1461–1471.
47. **Harhaj NS, Sun SC, Harhaj EW.** 2007. Activation of NF-kappaB by the human T cell leukemia virus type I Tax oncoprotein is associated with ubiquitin-dependent relocalization of IkappaB kinase. J. Biol. Chem. **282:** 4185–4192.
48. **Semmes OJ, Jeang KT.** 1996. Localization of human T-cell leukemia virus type 1 tax to subnuclear compartments that overlap with interchromatin speckles. J. Virol. **70:**6347–6357.
49. **Smith MR, Greene WC.** 1990. Identification of HTLV-I tax trans-activator mutants exhibiting novel transcriptional phenotypes. Genes Dev. **4:**1875–1885.
50. **Glickman MH, Ciechanover A.** 2002. The ubiquitin-proteasome proteolytic pathway: destruction for the sake of construction. Physiol. Rev. **82:** 373–428.
51. **Hemelaar J, Bex F, Booth B, Cerundolo V, McMichael A, Daenke S.** 2001. Human T-cell leukemia virus type 1 Tax protein binds to assembled nuclear proteasomes and enhances their proteolytic activity. J. Virol. **75:** 11106–11115.
52. **De Conto F, Pilotti E, Razin SV, Ferraglia F, Geraud G, Arcangeletti C, Scherrer K.** 2000. In mouse myoblasts nuclear prosomes are associated with the nuclear matrix and accumulate preferentially in the perinucleolar areas. J. Cell Sci. **113**(Part 13)**:**2399–2407.
53. **Sun SC, Elwood J, Beraud C, Greene WC.** 1994. Human T-cell leukemia virus type I Tax activation of NF-kappa B/Rel involves phosphorylation and degradation of I kappa B alpha and RelA (p65)-mediated induction of the c-rel gene. Mol. Cell. Biol. **14:**7377–7384.
54. **Fryrear KA, Guo X, Kerscher O, Semmes OJ.** 2012. The Sumo-targeted ubiquitin ligase RNF4 regulates the localization and function of the HTLV-1 oncoprotein Tax. Blood **119:**1173–1181.
55. **Huang J, Ren T, Guan H, Jiang Y, Cheng H.** 2009. HTLV-1 Tax is a critical lipid raft modulator that hijacks IkappaB kinases to the microdomains for persistent activation of NF-kappaB. J. Biol. Chem. **284:**6208–6217.
56. **Durkin SS, Guo X, Fryrear KA, Mihaylova VT, Gupta SK, Belgnaoui SM, Haoudi A, Kupfer GM, Semmes OJ.** 2008. HTLV-1 Tax oncoprotein

subverts the cellular DNA damage response via binding to DNA-dependent protein kinase. J. Biol. Chem. **283:**36311–36320.
57. **Lodewick J, Lamsoul I, Polania A, Lebrun S, Burny A, Ratner L, Bex F.** 2009. Acetylation of the human T-cell leukemia virus type 1 Tax oncoprotein by p300 promotes activation of the NF-kappaB pathway. Virology **386:**68–78.
58. **Lamsoul I, Lodewick J, Lebrun S, Brasseur R, Burny A, Gaynor RB, Bex F.** 2005. Exclusive ubiquitination and sumoylation on overlapping lysine residues mediate NF-kappaB activation by the human T-cell leukemia virus tax oncoprotein. Mol. Cell. Biol. **25:**10391–10406.
59. **Nasr R, Chiari E, El-Sabban M, Mahieux R, Kfoury Y, Abdulhay M, Yazbeck V, Hermine O, de The H, Pique C, Bazarbachi A.** 2006. Tax ubiquitylation and sumoylation control critical cytoplasmic and nuclear steps of NF-kappaB activation. Blood **107:**4021–4029.
60. **Durkin SS, Ward MD, Fryrear KA, Semmes OJ.** 2006. Site-specific phosphorylation differentiates active from inactive forms of the human T-cell leukemia virus type 1 Tax oncoprotein. J. Biol. Chem. **281:**31705–31712.
61. **El-Sabban ME, Nasr R, Dbaibo G, Hermine O, Abboushi N, Quignon F, Ameisen JC, Bex F, de The H, Bazarbachi A.** 2000. Arsenic-interferon-alpha-triggered apoptosis in HTLV-I transformed cells is associated with tax down-regulation and reversal of NF-kappa B activation. Blood **96:**2849–2855.
62. **El Hajj H, El-Sabban M, Hasegawa H, Zaatari G, Ablain J, Saab ST, Janin A, Mahfouz R, Nasr R, Kfoury Y, Nicot C, Hermine O, Hall W, de The H, Bazarbachi A.** 2010. Therapy-induced selective loss of leukemia-initiating activity in murine adult T cell leukemia. J. Exp. Med. **207:**2785–2792.
63. **Chase G, Deng T, Fodor E, Leung BW, Mayer D, Schwemmle M, Brownlee G.** 2008. Hsp90 inhibitors reduce influenza virus replication in cell culture. Virology **377:**431–439.
64. **Nakagawa S, Umehara T, Matsuda C, Kuge S, Sudoh M, Kohara M.** 2007. Hsp90 inhibitors suppress HCV replication in replicon cells and humanized liver mice. Biochem. Biophys. Res. Commun. **353:**882–888.
65. **Sun X, Bristol JA, Iwahori S, Hagemeier SR, Meng Q, Barlow EA, Fingeroth JD, Tarakanova VL, Kalejta RF, Kenney SC.** 2013. Hsp90 inhibitor 17-DMAG decreases expression of conserved herpesvirus protein kinases and reduces virus production in Epstein-Barr virus-infected cells. J. Virol. **87:**10126–10138.
66. **Yan P, Qing G, Qu Z, Wu CC, Rabson A, Xiao G.** 2007. Targeting autophagic regulation of NFkappaB in HTLV-I transformed cells by geldanamycin: implications for therapeutic interventions. Autophagy **3:**600–603.
67. **Trepel J, Mollapour M, Giaccone G, Neckers L.** 2010. Targeting the dynamic HSP90 complex in cancer. Nat. Rev. Cancer **10:**537–549.
68. **Ikebe E, Kawaguchi A, Tezuka K, Taguchi S, Hirose S, Matsumoto T, Mitsui T, Senba K, Nishizono A, Hori M, Hasegawa H, Yamada Y, Ueno T, Tanaka Y, Sawa H, Hall W, Minami Y, Jeang KT, Ogata M, Morishita K, Hasegawa H, Fujisawa J, Iha H.** 2013. Oral administration of an HSP90 inhibitor, 17-DMAG, intervenes tumor-cell infiltration into multiple organs and improves survival period for ATL model mice. Blood Cancer J. **3:**e132. doi:10.1038/bcj.2013.30.
69. **Takeda S, Maeda M, Morikawa S, Taniguchi Y, Yasunaga J, Nosaka K, Tanaka Y, Matsuoka M.** 2004. Genetic and epigenetic inactivation of tax gene in adult T-cell leukemia cells. Int. J. Cancer **109:**559–567.